IET Systems Biology

Research Article

IET Journals
The Institution of Engineering and Technology

Robust multi-objective blood glucose control in Type-1 diabetic patient

ISSN 1751-8849
Received on 24th September 2018
Revised 5th November 2018
Accepted on 16th November 2018
E-First on 20th March 2019
doi: 10.1049/iet-syb.2018.5093
www.ietdl.org

Sharmistha Mandal[1] ✉, *Ashoke Sutradhar*[2]

[1]*Electrical Engineering Department, Aliah University, Salt Lake, Kolkata, India*
[2]*Electrical Engineering Department, Indian Institute of Engineering Science and Technology, Howrah, India*
✉ *E-mail: itssharmistha@gmail.com*

Abstract: In this study, an automatic robust multi-objective controller has been proposed for blood glucose (BG) regulation in Type-1 Diabetic Mellitus (T1DM) patient through subcutaneous route. The main objective of this work is to control the BG level in T1DM patient in the presence of unannounced meal disturbances and other external noises with a minimum amount of insulin infusion rate. The multi-objective output-feedback controller with H_∞, H_2 and pole-placement constraints has been designed using linear matrix inequality technique. The designed controller for subcutaneous insulin delivery was tested on ***in silico*** adult and adolescent subjects of UVa/Padova T1DM metabolic simulator. The experimental results show that the closed-loop system tracks the reference BG level very well and does not show any hypoglycaemia effect even during the long gap of a meal at night both for ***in silico*** adults and adolescent. In the presence of 50 gm meal disturbance, average adult experience normoglycaemia 92% of the total simulation time and hypoglycaemia 0% of total simulation time. The robustness of the controller has been tested in the presence of irregular meals and insulin pump noise and error. The controller yielded robust performance with a lesser amount of insulin infusion rate than the other designed controllers reported earlier.

1 Introduction

Type-1 diabetes or insulin dependent diabetes mellitus is caused due to the insufficient insulin produced by the pancreas. The treatment of Type-1 diabetes is very challenging to the medical practitioners and engineers in terms of quantity of drug infused into the patient's blood stream and for maintaining the normal blood glucose (BG) level in the presence of various noises, uncertainties and patient parameter variations. An automated, continuous and controlled release of insulin to the bloodstream of a Type-1 Diabetes Mellitus (T1DM) patient is required to maintain *normoglycaemia* (BG level between 70 and 130 mg/dl on fasting and BG level not exceeding 140 mg/dl after 2 h of eating) in the presence of normal meal and activity conditions [1].

T1DM is a result of chronic autoimmune destruction of the pancreatic β-cells resulting in an absolute insulin deficiency. The glucose metabolism process is a non-linear complex process and is related to a number of internal factors, which are not always measurable. The system appears highly stochastic with accessible information like occasional BG sensing, amount of food intake and other activity conditions [1, 2].

The idea of artificial pancreas (AP) or closed-loop control for maintaining *normoglycaemia* in T1DM patient has been discussed by the researchers as to improve the diabetes management since the 1970s. The closed-loop AP consists of BG sensor, continuous subcutaneous (SC) insulin infusion pump and appropriate control algorithm. The closed-loop control of BG regulation involves the interplay between the non-linear dynamics of the physiological process, the inter-patient and intra-patient parameter variabilities, noises in the actuator (insulin pump) and in glucose sensor and other uncertainties. Robust regulation of glucose level is necessary for the patient's physiological process in the presence of meal disturbance, actuator and sensor noises. It is very difficult to establish *apriori,* the exact relationship amongst the interacting sub-processes due to dynamic non-linearities and parameter variations from patient to patient.

The insulin can be infused into the patient's body through intravenous (IV) route and SC route. Many researchers have developed a different mathematical model for designing the controller for controlling the BG in closed-loop fashion both through the IV and SC routes [2–5]. Researchers also worked on various closed-loop control algorithms for BG regulation [6–24] both through IV and SC routes. Parker *et al*. [6] designed an automatic H-infinity (H_∞) controller for controlling the BG level through the intravenous route considering Sorensen physiological model [3] and showed that controller tracks BG level very well. Dua *et al*. [12] developed a multi-objective controller based on Bergman's model [2] for BG regulation through intravenous route. Paoletti *et al*. [22] used Hovorka's model [4] for the design of data-driven robust model-predictive controller (MPC). Due to some inherent problems associated with IV insulin treatment, SC insulin therapy became very popular for BG regulation in T1DM patients and many control configurations such as proportional–integral–derivative (PID), linear quadratic Gaussian (LQG), H-infinity (H_∞), non-linear and MPC have been suggested [8–11, 13, 16–20, 23]. Among these H_∞ and MPC give a better result than the others. The motivation of this work is in the quest of design, analysis and synthesis of some robust controller for BG regulation in multivariable non-linear glycaemic process of T1DM patient with multiple constraints, where the design is based on a combination of more than one control objectives. The multi-objective control algorithm for BG regulation through SC route in T1DM patient has not reported earlier by any researcher.

In this study, a multi-objective controller is designed for BG regulation in TIDM patient through SC route applying linear matrix inequality (LMI) technique. The meal model developed by Man *et al.* [5] for the T1DM patient has been used and the controller is designed on linearised model of the TIDM subject. The designed controller has been tested on 22 *in silico* patients of UVa/Padova T1DM metabolic simulator [25] that is approved by the US Food and Drug Administration (FDA). The followings are the main contributions of this research work.

- This work applies the concept of designing an output-feedback multi-objective controller for BG regulation in T1DM patient to deliver insulin through SC route using LMI technique.
- The time-domain and frequency-domain design specifications such as H_∞ and H_2 performances and pole-placement constraints

have been set up for the glycaemic process in T1DM patients through the SC route.
- Multi-objective control algorithm has been developed with H_∞, H_2 and pole-placement constraints for BG regulation in T1DM patient through SC route.
- The designed multi-objective controller was tested on 11 *in silico* adult and also on 11 *in silico* adolescent subjects of T1DM simulator.

  ○ Experimental results show that the proposed controller regulates tightly the BG level in the presence of unannounced meal disturbances and also avoids hypoglycaemia effects. The insulin infusion required for BG regulation is also less.
  ○ The designed controller yielded a robust performance in the presence of irregular meals and pump error and noise. Here patients experience hypoglycaemia 0% of total simulation time.
  ○ The performance of the proposed multi-objective controller is compared with the performance of the H_∞ controller with safety mechanism (SM) and insulin feedback loop (IFL), tested on *in silico* adults in the T1DM simulator as reported in [19]. The proposed controller gives better performance with lesser hyperglycaemic and hypoglycaemic events and with a lesser amount of insulin infusion without using SM and IFL.
  ○ The performance of the designed controller is also compared with fully-automated online-tuned controller based on internal model control (IMC) strategy [23]. The designed multi-objective controller keeps the BG level of *in silico* patient more time within the clinically safe target zone (70–180 mg/dl) than this fully-automated online-tuned controller.

2 Glucose–insulin dynamics in Type-1 diabetics

The glucose–insulin kinetic model used in this work is based on the dynamic equations used by Dalla Man *et al.* [5] for the glucose-insulin process of T1DM patient with the meal simulation model. The closed-loop control scheme for BG regulation in T1DM patient with the meal simulation model, glucose sensor and insulin pump is shown in Fig. 1.

The meal model consists of a two-compartment glucose subsystem and two-compartment insulin subsystems. The SC insulin kinetics used in this study has been developed by Man *et al.* [9]; and SC glucose kinetics has been developed by Magni *et al.* [10]. This model has been successfully used by many researchers with *in silico* trials for testing various control algorithms [9–11, 13, 19, 20, 23]. The dynamic equations that represent the meal simulation model are given in the Appendix.

The block diagram of the patient model in an algebraic framework with inputs, outputs and feedback control is shown in Fig. 2, where $\boldsymbol{w}$ is the exogenous input vector consist of glucose reference, meal disturbance, actuator noise and sensor noise; u is the control input (insulin infusion); z_P is the BG level error, z_T is the plasma glucose level and z_u is the insulin infusion rate; y is the measured output (glucose level error).

The design specifications that have been considered to regulate the BG level of a T1DM patient using a multi-objective controller are

- To reject the effect of disturbances (meal disturbances, sensor and actuator noises).
- To minimise the postprandial BG concentration peak.
- To avoid the hypoglycaemia effect.
- To minimise the time required to settle down about the BG target.
- To minimise insulin infusion required from the SC insulin pump.

3 Multi-objective control via LMI technique

For the present problem, the design specifications are a combination of performances and robustness objectives and can be expressed both in the time and frequency domains. The multi-objective constraints are expressed regarding LMI and have also

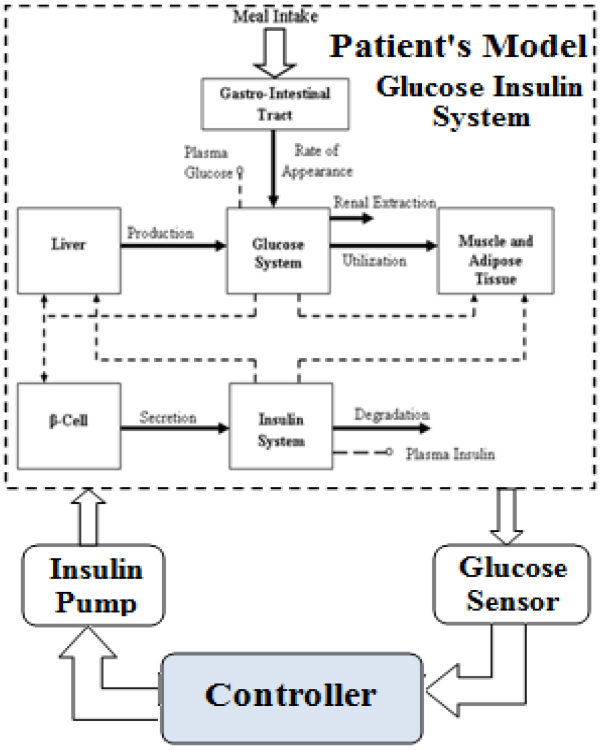

Fig. 1 *Closed-loop control scheme of glucose–insulin process*

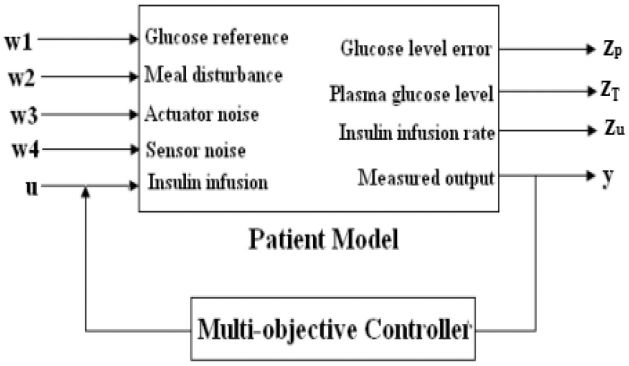

Fig. 2 *Block diagram of T1DM patient with the multi-objective controller*

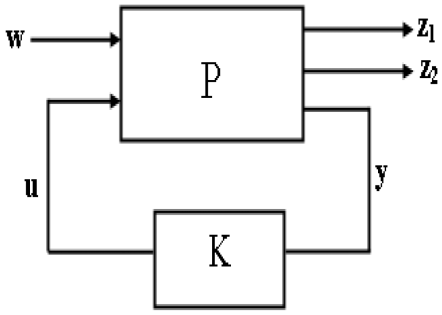

Fig. 3 *Process in an algebraic framework with the multi-objective controller*

been solved using LMI technique. The LMI technique is very popular for addressing the multi-objective problem. The various frequency and time-domain convex constraints such as H_∞ performance, H_2 performance and pole-placement [26–29] can be expressed as LMI and can be solved using convex optimisation algorithms.

Linear fractional transformation model of the closed-loop system is shown in Fig. 3 where P is the generalised plant and K is the multi-objective controller. The output vector z_1 is associated with H_∞ performance and output vector z_2 is associated with the H_2 performance. The output vectors are

$$z_1 = \begin{bmatrix} z_P & z_T & z_u \end{bmatrix}^{\mathrm{T}}; \quad z_2 = \begin{bmatrix} z_P & z_u \end{bmatrix}^{\mathrm{T}}$$

The state-space realisation of the plant P is

$$\dot{x}_P(t) = A_P \boldsymbol{x}_P(t) + B_{P1}\boldsymbol{w}(t) + B_{P2}u(t) \tag{1}$$

$$z_1(t) = C_{P1}\,\boldsymbol{x}_P(t) + D_{11}\boldsymbol{w}(t) + D_{12}u(t) \tag{2}$$

$$z_2(t) = C_{P2}\,x(t) + D_{21}\boldsymbol{w}(t) + D_{22}u(t) \tag{3}$$

$$y(t) = C_y x(t) + D_y \boldsymbol{w}(t) \tag{4}$$

where $\boldsymbol{x}_P(t)$ is the state vector of the plant, $\boldsymbol{w}(t)$ is the exogenous input vector, $u(t)$ is the control input and $y(t)$ is the measured output.

Here the objective is to design a multi-objective output feedback controller K to satisfy the robust stability and robust performance requirements, subject to the constraint that the closed-loop system is internally stable. Suppose the closed-loop transfer function of the system from w to z_1 and $\boldsymbol{w}$ to z_2 be $T_{z1\boldsymbol{w}}(s)$ and $T_{z2\boldsymbol{w}}(s)$, respectively, under output-feedback control $u = Ky$.

The state-space realisation of the controller is

$$\dot{x}_K = A_K \boldsymbol{x}_k(t) + B_K y(t) \tag{5}$$

$$u(t) = C_K \boldsymbol{x}_K(t) + D_K y(t) \tag{6}$$

where $\boldsymbol{x}_K(t)$ is state vector of the controller.

The state-space realisation of the closed-loop system as shown in Fig. 3 is given by

$$\dot{x}_C(t) = A_C \boldsymbol{x}_C(t) + B_C \boldsymbol{w}(t) \tag{7}$$

$$z_1(t) = C_{C1}\boldsymbol{x}_C(t) + D_{C1}\boldsymbol{w}(t) \tag{8}$$

$$z_2(t) = C_{C2}\boldsymbol{x}_C(t) + D_{C2}\boldsymbol{w}(t) \tag{9}$$

where $\boldsymbol{x}_C(t)$ is the state vector of the closed-loop system and is given by $x_C = \begin{bmatrix} x_P \\ x_K \end{bmatrix}$.

Here, for multi-objective output feedback control design, the controller gain K is computed such that it

- Minimises the trade-off criterion between H_2 and H_∞ norm of the following form:

$$J = \alpha T_{z1\boldsymbol{w}\infty}^2 + \beta T_{z2\boldsymbol{w}2}^2$$

  where $\alpha \succeq 0$, $\beta \succeq 0$ and $\alpha + \beta = 1$.
- Confines the closed-loop poles in some prescribed region in the left-half of the s-plane, called LMI region.

The H_∞ norm of $T_{z1\boldsymbol{w}}$ is less than any given γ where $\gamma \succ 0$ if there exists a positive symmetric P_∞ [28], such that the following LMI are feasible:

$$\begin{bmatrix} A_C P_\infty + P_\infty A_C^T & B_C & P_\infty C_C^T \\ B_C^T & -\gamma I & D_C^T \\ C_{C1}P_\infty & D_{C1} & -\gamma I \end{bmatrix} \prec 0, \quad P_\infty \succ 0 \tag{10}$$

The H_2 norm of $T_{z2\boldsymbol{w}}(s)$ is less than δ if and only if $D_{C2} = 0$ and if there exist positive symmetric P_2 and Q [28] such that the following LMI are feasible:

$$\begin{bmatrix} A_C P_2 + P_2 A_C^T & B_C \\ B_C^T & -I \end{bmatrix} \prec 0 \tag{11}$$

$$\begin{bmatrix} Q & C_C P_2 \\ P_2 C_C^T & P_2 \end{bmatrix} \succ 0 \tag{12}$$

$$\mathrm{trace}(Q) \prec \delta^2 \tag{13}$$

To improve the transient response, the closed-loop poles of the system can be confined in a prescribed region in the left-half of the s-plane called LMI region. An LMI region is a convex subset $\mathscr{D}$ of the complex plane [28] that is defined as

$$\mathscr{D} = \left\{ z \in C : \boldsymbol{L} + z\boldsymbol{M} + \bar{z}M^T \prec 0 \right\} \tag{14}$$

where $\boldsymbol{M}$ and $\boldsymbol{L} = L^T$ are the real matrices.

The closed-loop poles will be confined in the LMI region with $\boldsymbol{L} = L^T = \{\lambda_{ij}\}_{1 \le i,j \le m}$ and $\boldsymbol{M} = [\mu_{ij}]_{1 \le i,j \le m}$ if and only if there exits symmetric matrix $\boldsymbol{P}_{\mathrm{pol}}$ [28], which satisfies

$$\begin{bmatrix} \lambda_{ij}\boldsymbol{P}_{\mathrm{pol}} + \mu_{ij}A_C\boldsymbol{P}_{\mathrm{pol}} + \mu_{ij}\boldsymbol{P}_{\mathrm{pol}}A_C^A \end{bmatrix}_{1 < i,j < m} \prec 0, \quad \boldsymbol{P}_{\mathrm{pol}} \succ 0 \tag{15}$$

Here the multi-objective optimisation problem is non-convex because the matrix inequalities involved in (10), (11) and (15) are not jointly convex as $P_\infty \neq P_2 \neq P_{\mathrm{pol}}$. So it becomes very difficult to solve numerically the optimisation problem using LMI technique. The convexity can be recovered [28, 29] by seeking a common solution $P_\infty = P_2 = \boldsymbol{P}_{\mathrm{pol}} = P_C \succ 0$. The matrix inequalities in (10), (11) and (15) also contain non-linear terms, so the problem cannot be solved directly using the LMI technique. The non-linear problem can be converted into a linear one by changing the controller variables and the new controller variables are given by (16)–(19), where $\boldsymbol{R}$, $\boldsymbol{S}$, $\boldsymbol{M}$, $\boldsymbol{N}$ are the sub-matrices of P_C.

$$\begin{aligned} \bar{\boldsymbol{A}}_K = {} & \boldsymbol{N}A_K M^T + \boldsymbol{N}B_K C_y \boldsymbol{R} + \boldsymbol{S}B_{P2}C_K M^T \\ & + \boldsymbol{S}\left(A_P + B_{P2}D_K C_y\right)\boldsymbol{R} \end{aligned} \tag{16}$$

$$\overline{\boldsymbol{B}}_K = \boldsymbol{N}B_K + \boldsymbol{S}B_{P2}D_K \tag{17}$$

$$\overline{\boldsymbol{C}}_K = C_K M^T + D_K C_y \boldsymbol{R} \tag{18}$$

$$\overline{\boldsymbol{D}}_K = D_K \tag{19}$$

Once the new controller variables, $\bar{\boldsymbol{A}}_K$, $\overline{\boldsymbol{B}}_K$, $\overline{\boldsymbol{C}}_K$, $\overline{\boldsymbol{D}}_K$ and $\boldsymbol{R}$, $\boldsymbol{S}$, $\boldsymbol{M}$, $\boldsymbol{N}$ are obtained, the controller variables A_K, B_K, C_K and D_K can be determined by solving the equations from (16)–(19). The multi-objective output feedback controller K designed with the objectives mentioned earlier exits if and only if the following systems of LMIs are feasible:

$$\begin{bmatrix} \varnothing_{11} & \varnothing_{21}^T \\ \varnothing_{21} & \varnothing_{22} \end{bmatrix} \prec 0$$

where

$$\varnothing_{11} := \begin{bmatrix} A_P\boldsymbol{R} + \boldsymbol{R}A_P^T + B_{P2}\bar{\boldsymbol{C}}_K + \bar{\boldsymbol{C}}_K^T B_{P2}^T & B_{P1} + B_{P2}\bar{\boldsymbol{D}}_K D_y \\ \left(B_{P1} + B_{P2}\bar{\boldsymbol{D}}_K D_y\right)^T & -\gamma I \end{bmatrix}$$

$$\varnothing_{21} := \begin{bmatrix} \bar{\boldsymbol{A}}_K + \left(A_P + B_{P2}\bar{\boldsymbol{D}}_K C_y\right)^T & \boldsymbol{S}B_{P1} + \bar{\boldsymbol{B}}_K D_y \\ C_{P1}\boldsymbol{R} + D_{12}\bar{\boldsymbol{C}}_K & D_{11} + D_{22}\bar{\boldsymbol{D}}_K D_y \end{bmatrix}$$

$$\varnothing_{22} := \begin{bmatrix} A_P^T\boldsymbol{S} + \boldsymbol{S}A_P + \bar{\boldsymbol{B}}_K C_y + C_y^T \bar{B}_K^T & \left(C_{P1} + D_{12}\bar{\boldsymbol{D}}_K C_y\right)^T \\ C_{P1} + D_{12}\bar{\boldsymbol{D}}_K C_y & -\gamma I \end{bmatrix}$$

and

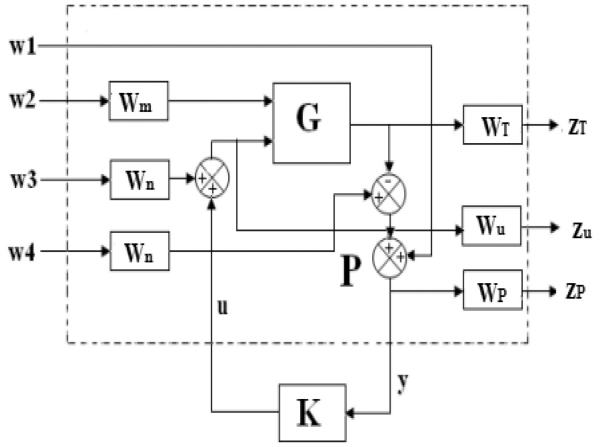

Fig. 4 *T1DM patient under multi-objective output-feedback control*

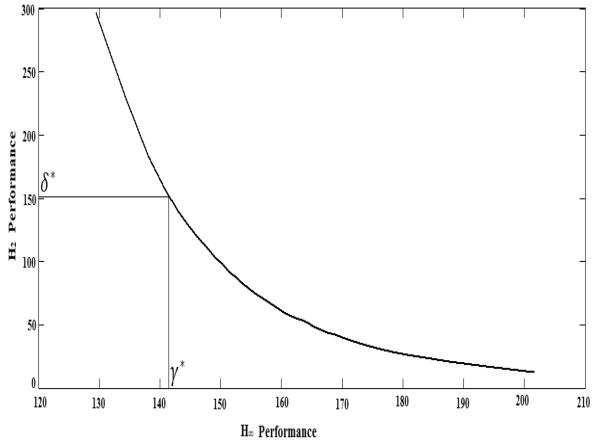

Fig. 5 *Multi-objective trade-off curve for the GI process*

$$\begin{bmatrix} Q & C_{P2}\boldsymbol{R} + D_{22}\bar{\boldsymbol{C}}_K & C_{P2} + D_{22}\bar{\boldsymbol{D}}_K C_y \\ \left(C_{P2}\boldsymbol{R} + D_{22}\bar{\boldsymbol{C}}_K\right)^T & \boldsymbol{R} & I \\ \left(C_{P2} + D_{22}\bar{\boldsymbol{D}}_K C_y\right)^T & I & \boldsymbol{S} \end{bmatrix} \succ 0$$

(see equation below). Along with $\text{trace}(Q) < \delta_0^2$

$$\gamma^2 \prec \gamma_0^2$$

$$D_{21} + D_{22}\bar{\boldsymbol{D}}_K D_y = 0$$

The matrices $\boldsymbol{R} = R^T \in \mathscr{R}^{n\times n}$, $\boldsymbol{S} = S^T \in \mathscr{R}^{n\times n}$ and matrices $\bar{\boldsymbol{A}}_K$, $\bar{\boldsymbol{B}}_K$, $\bar{\boldsymbol{C}}_K$, $\bar{\boldsymbol{D}}_K$ can be determined by solving the above LMIs. If the optimal solutions of the above LMI problem are γ^* and Q^*, then the closed-loop H_∞ and H_2 performances are bounded by $T_{z1w\infty} \preceq \gamma^*$, $T_{z2w2} \preceq \sqrt{\text{trace}(Q^*)}$, where the closed-loop poles are confined in the prescribed LMI region $\mathscr{D}$. The matrix elements $\boldsymbol{\lambda}_{ij}$ and $\boldsymbol{\mu}_{ij}$ are related to the prescribed LMI region $\mathscr{D}$.

4 Multi-objective controller design for the glucose–insulin process

The non-linear model of glucose–insulin process in SC route for T1DM patient based on the dynamic equations given in the Appendix is implemented using MATLAB SIMULINK® toolboxes and the model is linearised around the target value of glucose concentration (120 mg/dl) assuming no disturbances. The order of the linearised model is 16th. Fig. 4 shows the control configuration for the T1DM patient with weighting functions and multi-objective controller K.

In Fig. 4, W_m represents meal disturbance weight. The meal disturbances are considered as rectangular pulses. To make a smooth rise and fall of the meal disturbance pulses that happen to the subject [6], these signals are passed through a first-order low-pass filter W_m. Depending on the absorption of disturbance dynamics in the patient's physiological process, the time constant of W_m has been selected. For the present glucose–insulin process, the low-pass filter W_m is considered as $W_m = (1/(4s+1))$.

The weights for both actuator and sensor noise are taken as $W_n = 0.0001$. The noise signals are considered Gaussian in nature and the intensity depends on the statistics of error in the device outputs.

In Fig. 4, Wu is the control input weight and the performance weights are W_P and W_T. The W_P, W_T and W_u are used for shaping the performances of closed-loop process. Here the objective for the problem is to minimise the sensitivity function S, KS and complementary sensitivity function T. For the glucose–insulin process, the weight functions W_P, W_T and W_u are chosen as

$$W_P(s) = \frac{s/M_P + \omega_P}{s + \omega_P A_P} = \frac{0.6667s + 0.9}{s + 0.0009}$$

$$W_T(s) = \frac{s + \omega_T/M_T}{A_T s + \omega_T} = \frac{s + 0.001}{0.001s + 0.001}$$

$$W_u(s) = \left(\frac{s + \omega_u/\sqrt[2]{M_u}}{\sqrt[2]{A_u}s + \omega_u}\right)^2 = \frac{1111s^2 + 54.43s + 0.6667}{1.111s^2 + 2.108s + 1}$$

After selection of the weight functions, the Pareto-like trade-off curve is determined using LMI technique and by minimising the trade-off criterion between H_2 and H_∞ norm of the form $\{J = \min(\boldsymbol{\alpha\gamma}^2 + \boldsymbol{\beta\delta}^2)\}$ for each value α and β between 0 and 1, where $\alpha \geq 0$, $\beta \geq 0$ and $\alpha + \beta = 1$. The trade-off curve is shown in Fig. 5. From this trade-off curve, the best values of H_∞ and H_2 norm are obtained as $\gamma^* = 142.11$ and $\delta^* = 152.02$, respectively, and these values are achieved for $\alpha = 0.887$ and $\beta = 0.113$. Control algorithm has been implemented using MATLAB LMI control Toolbox.

The flowchart of the proposed control algorithm is shown in Fig. 6. To improve the transient response of the process or to provide damping, the closed-loop poles of the output feedback system had been placed in a prescribed LMI region as shown in Fig. 7. The region is chosen as the conic sector with the apex at $x = 0$ and angle $\theta = 5^\circ$.

5 Results and discussion

The performance of the designed multi-objective controller is tested *in silico* subjects of UVa/Padova T1DM simulator v3.2 that is accepted by the FDA in connection with the development of AP. The simulator has three different groups of *in silico* subjects; children, adolescent and adults. In each group, there are 11 subjects (10 different subjects and 1 average). Each subject has a different age, body weight and other parameters [25]. Using the simulator an optimal bolus insulin dose can be provided for a given meal size to each subject based on the subject's basal rate and insulin-to-carbohydrate ratio (I:C). The proposed controller has been tested on 11 *in silico* adult and 11 *in silico* adolescents with different meal size, errors and noises in an insulin pump. Continuous glucose monitor (CGM) is taken for glucose sensing and continuous SC insulin infusion (CSII) pump is chosen for insulin infusion into the body of the patient in this simulator.

$$\left[\lambda_{ij}\begin{pmatrix}\boldsymbol{R} & I\\ I & \boldsymbol{S}\end{pmatrix} + \mu_{ij}\begin{pmatrix}A_P\boldsymbol{R} + B_{P2}\bar{\boldsymbol{C}}_K & A_P + B_{P2}\bar{\boldsymbol{D}}_K C_y\\ \bar{A}_K & \boldsymbol{S}A_P + \bar{\boldsymbol{B}}_K C_y\end{pmatrix} + \mu_{ji}\begin{pmatrix}\boldsymbol{R}A_P^T + \bar{C}_K^T B_{P2}^T & \bar{A}_K^T\\ \left(A_P + B_{P2}\bar{\boldsymbol{D}}_K C_y\right)^T & A_P^T\boldsymbol{S} + C_y^T\bar{B}_K^T\end{pmatrix}\right]_{1\leq i,j\leq m} \prec 0$$

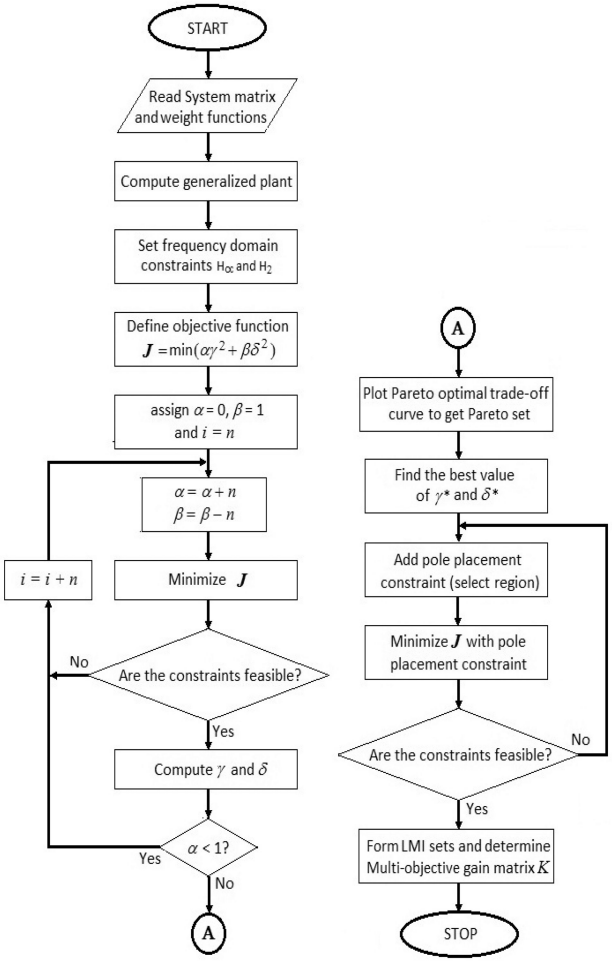

Fig. 6 *Flowchart of the proposed control algorithm*

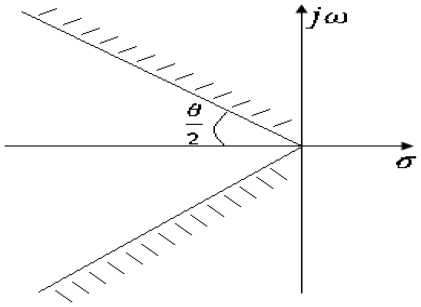

Fig. 7 *Prescribed LMI region*

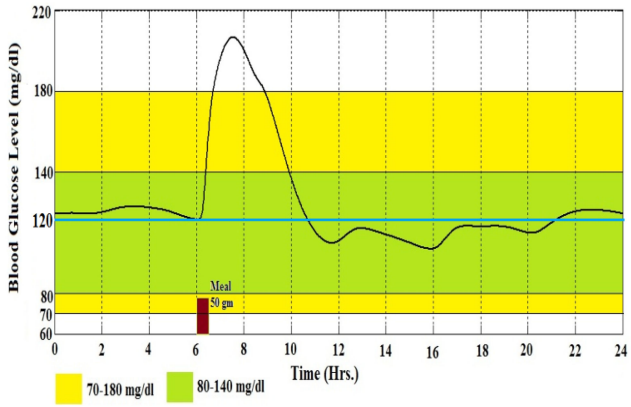

Fig. 8 *BG level of an adult-average when subjected to 50 gm meal (green shaded region represents the euglycemic zone and the yellow one represents the normoglycaemic zone)*

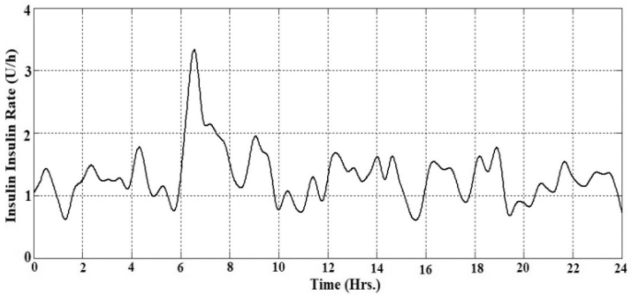

Fig. 9 *Insulin infusion rate of an adult-average when subjected to 50 gm meal*

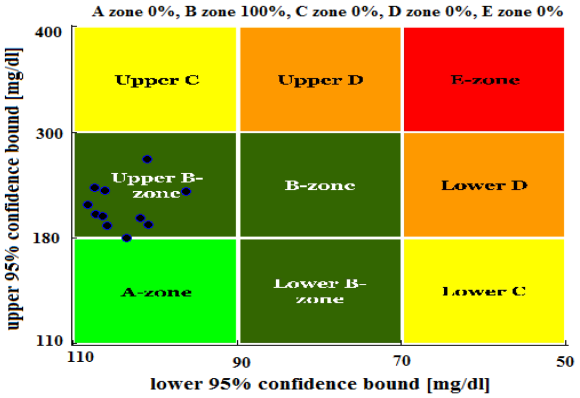

Fig. 10 *CVGA plot for 11 in silico adults*

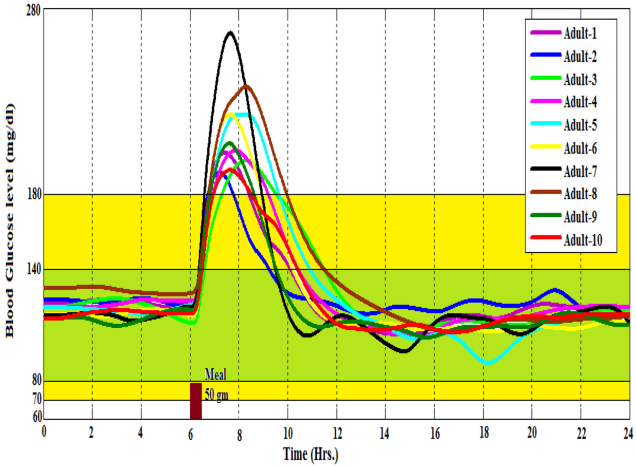

Fig. 11 *BG response of adult-avg. when subjected to 50 gm meal*

5.1 Testing on in silico adults

For testing the multi-objective controller in this tracking problem, the target value of plasma glucose concentration is considered as 120 mg/dl because this target value is frequently used in clinical trials [8]. The controller has been tested on *in silico* adults in the presence of unannounced meal disturbances with CGM glucose sensor and an insulin pump with no error. One day (24 h) simulation time is considered and the simulation is started at midnight where the controller is turned ON at the same time. A single meal of 50 g CHO is subjected to all adults (11) after 6 h of starting the simulation. The BG level and insulin infusion rate profiles of adult-average are shown in Figs. 8 and 9, respectively. From the responses and results, the followings can be observed:

- Postprandial BG concentration peak is within clinically safe normoglycaemic BG zone of 70–180 mg/dl and BG level of adult avg. remains 92% of the time within this zone.
- The minimum BG level observed is 98 mg/dl and hence the hypoglycaemia effect is not noticed.

Table 1 Average results for 11 *in silico* adult subjects of theUVa/Padova simulator with a meal of 50 gm

Adult ID	Mean BG, mg/dl	Peak BG, mg/dl	Mean post-meal BG	Min. BG, mg/dl	%Time <70 mg/dl	%Time in target 70–180 mg/dl	%Time within 80–140 mg/dl
1	121.7	202	199	106	0	93.2	85.5
2	122.7	192	180	118	0	97.2	89.3
3	128.9	198	189	110	0	89.1	79.8
4	122.7	204	188	105	0	92	84.1
5	128.3	222	216	90	0	87.2	82
6	124.4	223	225	107	0	90.3	85.1
7	127	267	264	96	0	89.5	87.5
8	134.8	238	216	109	0	87	79.9
9	123.5	208	211	108	0	92.3	87.5
10	123.6	193	190	108	0	93.4	84.4
avg	124.4	207	200	98	0	92	85.4

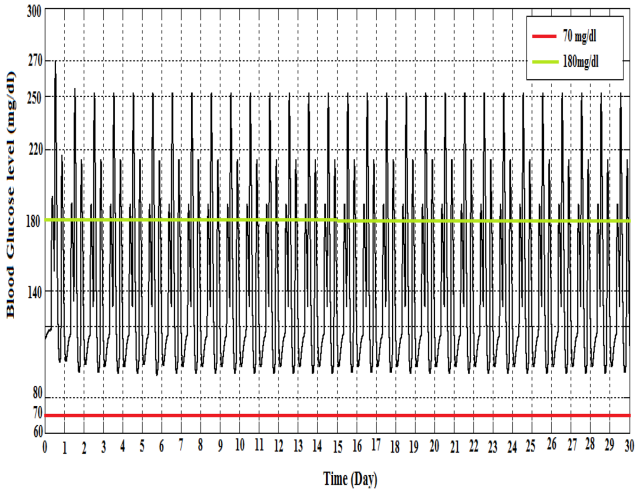

Fig. 12 *BG response through 30-days of adult-average when subjected to multi-meal*

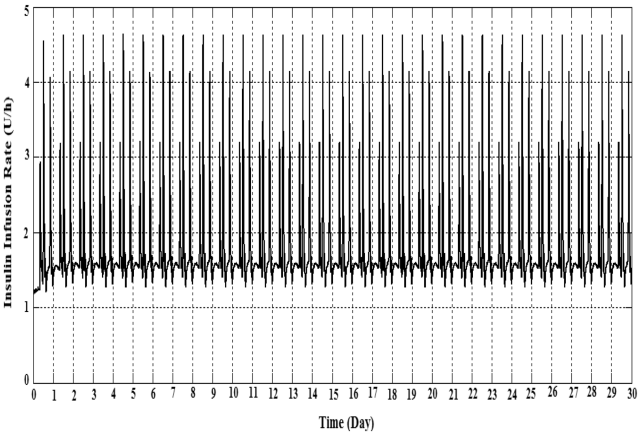

Fig. 13 *Insulin infusion rate through 30-days of adult-average when subjected to multi-meal*

- A minimal High BG Index (HBGI = 1.45), a minimal Low BG Index (LBGI = 0) and BG Risk Index (BGRI = 1.46) have been achieved.
- The insulin infusion rate response shows that maximum 3.3 U/h insulin is required to regulate the BG level, which is very much less.

The control variability grid analysis (CVGA) plot of all 11 adults is shown in Fig. 10. Each blue dot represents each adult's minimum and maximum BG level. From the plot, it is also observed that the clustering of points of all adults is tighter and is placed in upper B-zone. The BG responses of 11 *in the silico* adult

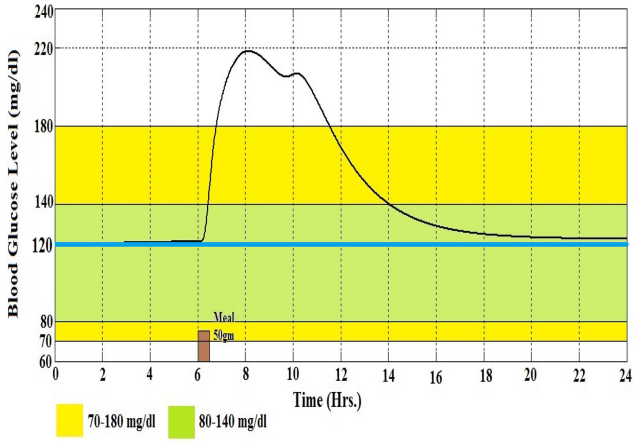

Fig. 14 *BG response in adolescent-average when subjected to 50 gm meal*

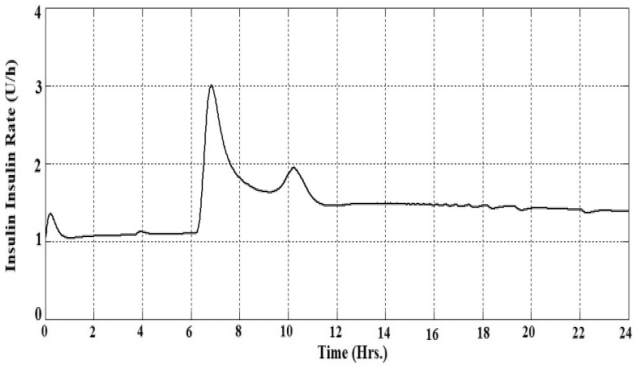

Fig. 15 *Insulin infusion rate in adolescent-average when subjected to 50 gm meal*

of the simulator with 50 gm meal are given in Fig. 11 and average results are given in Table 1.

The designed controller is also tested through 30-days. Here repetitive diets have been followed and patient consumes three meals in a day (at 07:00 h, 12:00 h and 20:00 h) with a fixed amount of CHO (40, 75, 60 gm respectively). The 30-day BG level and insulin infusion responses are shown in Figs. 12 and 13, respectively. The BG response shows that hypoglycaemia effect is absent in the response. It also shows that the first-day peak BG level is 270 mg/dl for 75 gm meal and from the Day-4, the maximum BG level remains almost fixed within 250 mg/dl. From the insulin infusion rate, it is seen that for 75 gm meal the insulin infusion rate is only 4.5 U/h.

5.2 Testing on in silico adolescents

The proposed controller has also been tested on *in silico* adolescents. The 24 h simulation time is considered and the simulation is started at midnight where the controller is turned ON

Table 2 Average results for 11 *in silico* adolescent subjects of the UVa/Padova simulator with a meal of 50 gm

Adolescent ID	Mean BG, mg/dl	Mean post-meal BG	%Time <70 mg/dl	%Time >300 mg/dl	%Time in target 70–180 mg/dl	%Time above 70–180 mg/dl
1	121.7	254.6	0	0	89.52	10.48
2	130.5	256.27	0	0	90.08	9.92
3	134.3	216.72	0	0	88.97	11.03
4	142.2	251.91	0	0	81.96	18.04
5	151.5	206.89	0	0	76.89	23.11
6	140.2	208.63	0	0	83.55	16.45
7	142.4	272.79	0	0	84.94	15.06
8	138.2	214.5	0	0	81.75	18.25
9	143.8	209.28	0	0	80.22	19.78
10	136.6	204.53	0	0	85.84	14.16
avg	133.2	231.56	0	0	86.47	13.53

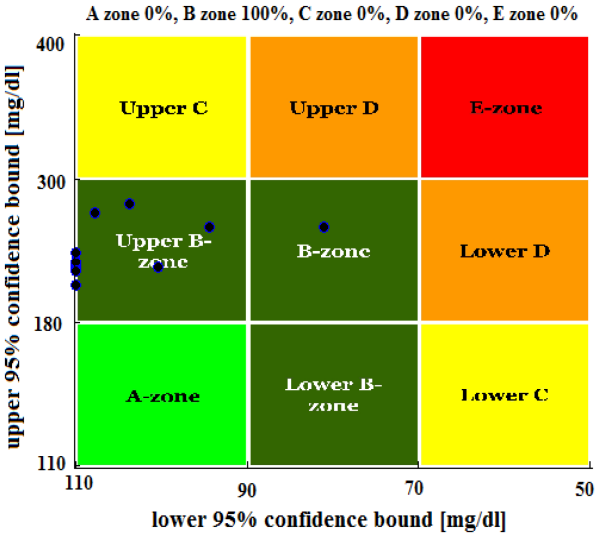

Fig. 16 *CVGA plot for 11 in silico adolescent*

Table 3 Meal time and meal size

	Time	8 h	12 h	8 h
Day 1	size, gm	45	75	70
Day 2	size, gm	50	—	90
Day 3	size, gm	—	—	—
Day 4	size, gm	50	80	60

at the same time. All adolescents (11) are subjected to a single meal of 50 g CHO after 6 h of starting the simulation with CGM glucose sensor and an insulin pump with no error. The BG and insulin infusion rate profiles of the average subject are shown in Figs. 14 and 15, respectively. The average results of the subjects are shown in Table 2. From the results and responses, the followings can be observed:

- Hypoglycaemia effect is absent and the postprandial BG concentration peak is also within the clinically safe *normoglycaemic* BG zone of 70–180 mg/dl.
- BG level of the average subject remains 86.47% of the time within the *normoglycaemic* zone of 70–180 mg/dl.
- The time required to settle down about the target value is more than the time required for an average adult.
- The insulin infusion rate response shows that controller delivers a maximum of 3 U/h insulin to regulate the BG level for 50 gm meal.

So the controller fulfils the objectives for BG regulation via the SC route for adolescents also. Further tuning of the controller may be required for using with adolescents. The CVGA plot of all adolescents is shown in Fig. 16. From the plot, it can also be

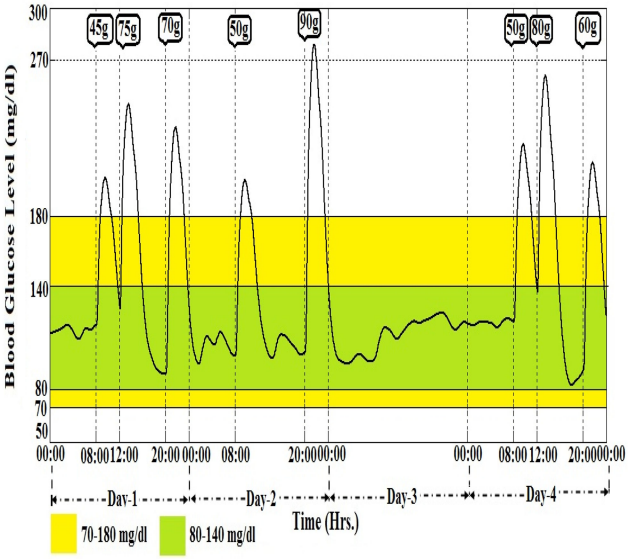

Fig. 17 *BG response of adult-average when subjected to irregular meals*

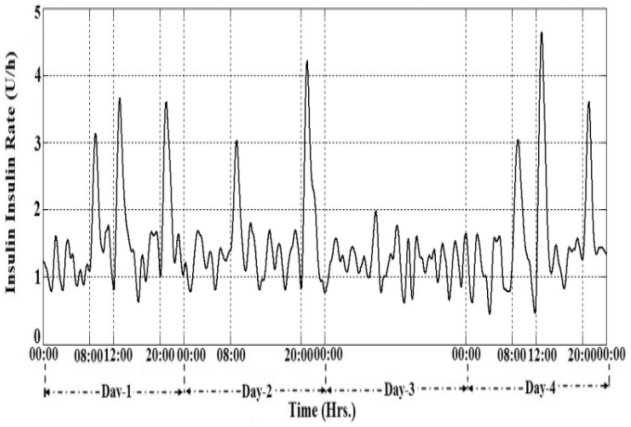

Fig. 18 *Insulin infusion rate of adult-average when subjected to irregular meals*

observed that the clustering of points of all adolescents is tighter and are in upper B-zone and B-zone.

5.3 Robustness analysis

- *Case 1:* For robustness, the controller is tested through 4-days when the patient was subjected to irregular meals. The meal size and meal time are given in Table 3. Here on Day 2, the patient skipped the lunch and on Day 3, the patient was on fasting. The BG level and insulin infusion rate responses are shown in Figs. 17 and 18, respectively. From the response, it is observed

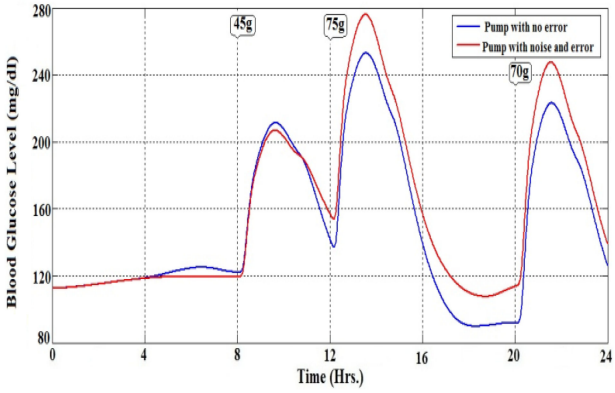

Fig. 19 *BG response in adult-average with and without insulin pump noise and error*

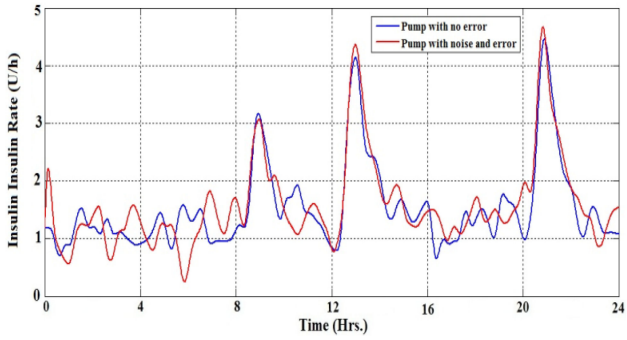

Fig. 20 *Insulin infusion rate in adult-average with and without insulin pump noise and error*

that the postprandial BG level is <180 mg/dl, i.e. in the safe region. Even on day-3, when the patient is on fasting the BG level is in a euglycaemic zone. So the controller tracks the target value very well and the overnight *hypoglycaemia* effect cannot be noticed. The insulin requirements are also very less as evident from the figure. So the proposed controller regulates BG robustly with the minimum drug.

- *Case 2:* For robustness analysis, the simulation is also carried out in the presence of insulin pump noise and error (i.e. in built noise and error in T1DM simulator). The simulation time is taken as 24 h. The subject is given 45 gm a meal at 08:00 h, 75 gm meal at 12:00 h and 70 gm meal at 20:00 h. The BG and insulin infusion responses with pump noise, error and without pump noise, error are given in Figs. 19 and 20, respectively. From the red BG curve, it can be observed that the postprandial BG level is within a clinically safe region (70–180 mg/dl) and hypoglycaemia effect is also not obtained. From the insulin infusion curves, it is clear that the insulin requirements in both the cases are almost the same. Thus the controller regulates the BG very well in the presence of meal disturbances as well as insulin pump noise, error with almost the same amount of insulin. Thus the controller gives a robust performance in the presence of pump noise and error also.

5.4 Performance comparison with other controllers from earlier reports

- *Case 1:* The performance of the proposed multi-objective controller is compared with the performance of H_∞ controller with SM and IFL, tested on *in silico* 101 adults in T1DM simulator as reported in [19]. The patient was subjected to the same meal regimen considered in [19] and is given in Table 4. The BG target is taken as 120 mg/dl and the comparative average performance of the proposed controller with that of the reported in [19] are given in Table 5 for meal Protocol #1 and Protocol #2. From the results, the followings can be seen:

  ○ Designed multi-objective controller avoids hypoglycaemia effect without using SM and IFL as used with H_∞ controller reported in [19].
  ○ From Table 5, it can be seen that the postprandial BG, mean BG and maximum BG level all are less than the H_∞ controller reported in [19].
  ○ The percentage time in target value (70–180 mg/dl) is also more in case multi-objective controller.
  ○ The maximum insulin infusion rate required for the multi-objective controller is very much less than this H_∞ controller and that is another advantage of this proposed multi-objective controller.
- Thus the proposed controller gives better performance with lesser hyperglycaemic and hypoglycaemic events and with a lesser amount of insulin infusion without using SM and IFL.

Table 4 Meal time and sizes as given in [19]

		Meal protocol #1			Meal protocol #2		
		Day 1	Day 2	Day 3	Day 1	Day 2	Day 3
breakfast	time	7 am	6 am	7 pm	7 pm	—	7 pm
	size, gm	50	50	50	50	—	50
lunch	time	2 pm	1 pm	1 pm	—	12 pm	2 pm
	size, gm	60	70	65	—	55	55
dinner	time	8 pm	7 pm	9 pm	8 pm	9 pm	8 pm
	size, gm	50	50	55	60	50	50

Table 5 Comparison of controller responses with meal protocols and controller strategies [19]

Controller performance	Protocol #1			Protocol #2		
	As reported in [19] postprandial (PP)	As reported in [19] overall (O)	Proposed controller	As reported in [19] postprandial (PP)	As reported in [19] overall (O)	Proposed controller
mean BG	176	148	138.08	177	154	134.5
max. BG	229	226	228	224	220	222
min. BG	108	96	86	114	108	98
%time in [70–180 mg/dl]	54.2	75.9	77.51	54.4	75.5	79.43
%time in >300	0.3	0.1	0	0.1	0	0
%time in >180	45.8	24	22.49	45.6	24.5	20.57
%time in <70	0	0.1	0	0	0	0
max. insulin infu. rate, U/h	7	—	3.8	6	—	4

Table 6 Meal time and sizes as given in [23]

Scenario	Simulation time	Start time of simulation	Number of meal disturbances	Administration of meal time and size
scenario 1	24 h	3:00 am	3	two 75 gm at 7:00 am and 1:00 pm. One 50 gm at 8:00 pm.

Table 7 Comparison of controller performance with IMC algorithms [23] for Scenario 1

Performance metrics	Offline-tuned IMC	Online-tuned IMC	Semi-automated online-tuned IMC	**Proposed controller**
mean	177.41	172.47	115.12	**126.36**
%time in normoglycaemia (70–180 mg/dl)	56.83	59.35	94.1	**94.26**
%time in tight target (80–140 mg/dl)	37.17	38.51	72.39	**72.67**
%time below70 mg/dl	0	0	3.54	**0**
%time above 180 mg/dl	43.16	40.64	2.34	**5.74**
LBGI	0.025	0.026	1.15	**0.16**
HBGI	9.31	8.75	0.83	**1.39**

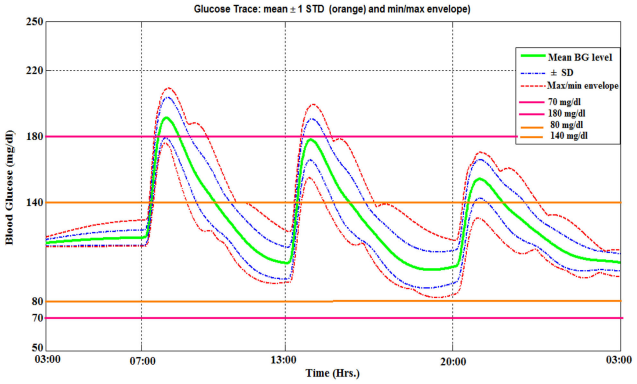

Fig. 21 *Mean BG response of adult avg. (green solid line), SD (blue dotted line) and min/max. envelop (red dotted line) for Scenario 1*

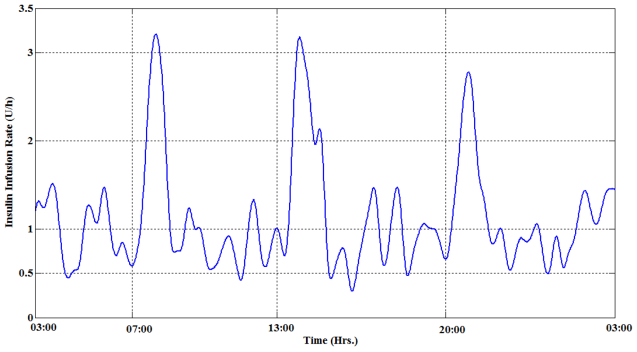

Fig. 22 *Insulin infusion rate of avg. adult (blue dotted line) for Scenario 1*

- *Case 2:* The performance of the proposed controller is also compared with the performance of fully-automated offline- and online tuned IMC and semi-automated online-tuned IMC [23]. The patient was subjected to the same meal disturbances as in scenario 1 [23] and is given in Table 6.
- The BG target is taken as 110 mg/dl as in [23]. The comparative average performance of the proposed controller with that of the reported in [23] is given in Table 7 for scenario 1. The BG and insulin infusion rate are given in Figs. 21 and 22. The percentage time in target value (70–180 mg/dl) and percentage time in tight target (80–140 mg/dl) is also more in case multi-objective controller. Percentage time below 70 mg/dl is also zero. So the proposed controller gives better result than the controllers reported in [23].

6 Conclusion

In this paper, a multi-objective control algorithm using LMI technique has been proposed for closed-loop robust BG regulation in T1DM patient through SC route. For convex stabilisation of the insulin delivery system, multi-objective constraints H_∞, H_2, and pole-placement have been expressed regarding LMI. The designed multi-objective controller is tested on *in silico* subjects of UVa/Padova T1DM Simulator v3.2 in the presence of meal disturbances and insulin pump noise and error. The control algorithm is validated on *in silico* 11 adults and 11 adolescents. The controller response shows no postprandial hyperglycaemia and hypoglycaemia effects and regulates the BG level with minimum amount of insulin infusion, which is very much desired for AP application. For robustness analysis, the proposed multi-objective controller was tested on *in silico* adults and adolescents, with irregular meals and with and without insulin pump error and noises. The resulting controller yielded robust performance with less amount of insulin infusion even in the presence of irregular meals and pump error and noise. This controller regulates the BG level very tightly with minimum control effort and does not require any bolus insulin feedback loop as reported in earlier research work.

The limitations of this work are that the effects of counter-regulatory hormones such as glucagon, growth hormones and so on have not been considered in the model of glucose–insulin process and also the effects of physical exercise by the patient is not considered. In future, the performance of the multi-objective controller with proper exercise and activity model may be studied on *in silico* patients.

7 References

[1] Nathan, D.M.: 'The diabetes control and complications trial/epidemiology of diabetes interventions and complications study at 30 years: overview', *Diabetes Care*, 2014, **37**, pp. 9–16

[2] Bergman, R.N., Phillips, L.S., Cobelli, C.: 'Physiologic evaluation of factors controlling glucose tolerance in man: measurement of insulin sensitivity and, β-cell glucose sensitivity from the response to intravenous glucose', *J. Clin. Invest*, 1981, **68**, (6), pp. 1456–1467

[3] Sorensen, J.T.: 'A physiologic model of glucose metabolism in man and its use to design and assess improved insulin therapies for diabetes', Ph.D. thesis, Department of Chemical Engineering, MIT, April 1985

[4] Hovorka, R., Canonico, V., Chassin, L.J., *et al.*: 'Nonlinear model predictive control of glucose concentration in subjects with type1 diabetes', *Physiol. Meas.*, 2004, **25**, (4), pp. 905–920

[5] Man, C.D., Rizza, R.A., Cobelli, C.: 'Meal simulation model of the glucose-insulin system', *IEEE Trans. Biomed. Eng.*, 2007, **54**, (10), pp. 1740–1749

[6] Parker, R.S., Doyle, F.J., Ward, J.H., *et al.*: 'Robust H_∞ glucose control in diabetes using a physiological model', *Bioeng., Food, Natl. Prod.*, 2000, **46**, (12), pp. 2537–2549

[7] Sutradhar, A., Chaudhuri, A.S.: 'Design and analysis of an optimally convex controller in algebraic framework for a micro-insulin dispenser system', *J. AMSE, France, Adv. Model. Anal. C*, 2002, **57**, (1–2), pp. 1–14

[8] Steil, G.M., Rebrin, K., Darwin, C., *et al.*: 'Feasibility of automating insulin delivery for the treatment of type 1 diabetes', *Diabetes*, 2006, **55**, (12), pp. 3344–3350

[9] Man, C.D., Raimondo, D.M., Rizza, R.A., *et al.*: 'GIM simulation software of meal glucose–insulin model', *J. Diabetes Sci. Technol.*, 2007, **1**, (3), pp. 323–330

[10] Magni, L., Raimondo, D.M., Bossi, L., *et al.*: 'Model predictive control of type 1 diabetes: an in silico trial', *J. Diabetes Sci. Technol.*, 2007, **1**, (6), pp. 804–812

[11] Patek, S.D., Breton, M.D., Chen, Y., *et al.*: 'Linear 1uadratic Gaussian-based closed-loop control of type 1 diabetes', *J. Diabetes Sci. Technol.*, 2007, **1**, (6), pp. 834–841

[12] Dua, P., Doyle, F.J., Pistikopoulos, E.N.: 'Multi-objective blood glucose control for type 1 diabetes', *Med. Biol. Eng. Comput.*, 2009, **47**, (3), pp. 343–352

[13] Kovatchev, B.P., Breton, M., Man, C.D., *et al.*: 'In silico preclinical trials: a proof of concept in closed-loop control of diabetes', *J. Diabetes Sci. Technol.*, 2009, **3**, (1), pp. 44–55

[14] Mandal, S., Sutradhar, A.: 'Blood glucose regulation in IDDM patient by H∞ control: an LMI approach'. Proc. of the Int. Conf. on Systems in Medicine

and Biology (ICSMB 2010), IIT Kharagpur, India, 2010, DOI: 10.1109/ICSMB.2010.5735405
[15] Mandal, S., Sutradhar, A.: 'LMI based robust blood glucose regulation in type-1 diabetes patient with multi-meal ingestion', *J. Inst. Eng. (India), B*, 2014, **95**, (2), pp. 121–128
[16] Wang, Y., Dassau, E., Doyle, F.J.: 'Closed-loop control of artificial pancreatic β-cell in type 1 diabetes mellitus using model predictive iterative learning control', *IEEE Trans. Biomed. Eng.*, 2010, **57**, (2), pp. 211–219
[17] Lee, J.B., Dassau, E., Seborg, D.E., *et al.*: 'Model-based personalization scheme of an artificial pancreas for type 1 diabetes applications'. American Control Conf. (ACC), Washington, DC, USA, 2013, pp. 2911–2916
[18] Lee, J.J., Dassau, E., Zisser, H., *et al.*: '*In silico* evaluation of an artificial pancreas combining exogenous ultrafast-acting techno sphere insulin with zone model predictive control', *J. Diabetes Sci. Technol.*, 2013, **7**, (1), pp. 215–226
[19] Colmegna, P., Śanchez Pe˜na, R.S., Gondhalekar, R., *et al.*: 'Reducing risks in type 1 diabetes using $H\infty$ control', *IEEE Trans. Biomed. Eng.*, 2014, **61**, (12), pp. 2939–2947
[20] Bhattacharjee, A., Sutradhar, A.: 'Data driven nonparametric identification and model based control of glucose-insulin process in type-1 diabetics', *J. Process Control*, 2016, **41**, pp. 14–25
[21] Mandal, S., Sutradhar, A.: 'Multi-objective control of blood glucose with H_∞ and pole-placement constraints', *Int. J. Dyn. Control*, 2017, **5**, (2), pp. 357–366
[22] Paoletti, N., Liu, K.S., Smolka, S.A., *et al.*: 'Data-driven robust control for type 1 diabetes under meal and exercise uncertainties'. Int. Conf. on Computational Methods in Systems Biology CMSB, 2017, pp. 214–232, DOI: 10.1007/978–3–319–67471–1_13
[23] Bhattacharjee, A., Easwaran, A., Leow, M.K.-S., *et al.*: 'Evaluation of an artificial pancreas in *In silico* patients with online-tuned internal model control', *Biomed. Signal Proc. Control*, 2018, **41**, pp. 198–209
[24] Bequette, B.W.: 'Challenges and recent progress in the development of a closed-loop artificial pancreas', *Annu. Rev. Control*, 2012, **36**, (2), pp. 255–266
[25] UVa/padova T1DMS simulator type-1 diabetes metabolic simulator, user guide v3.2, TEG The Epsilon Group, April 14, 2014
[26] Boyd, S., Ghaoui, L., Feron, E., *et al.*: '*Linear matrix inequalities in system and control theory*' (SIAM, Philadelphia, 1994), vol. **15**
[27] Gahinet, P., Nemirovski, A., Laub, A., *et al.*: '*The LMI control toolbox*' (The Mathworks, Natick, MA, 1995)
[28] Chilali, M., Gahinet, P.: 'H_∞ design with pole placement constraints: an LMI approach', *IEEE Trans. Autom. Control*, 1996, **41**, (3), pp. 358–367
[29] Scherer, C., Gahinet, P., Chilali, M.: 'Multiobjective output-feedback control via LMI optimization', *IEEE Trans. Autom. Control*, 1997, **42**, (7), pp. 896–911

8 Appendix

8.1 Dalla-Man model of glucose–insulin dynamics in Type-1 diabetics

The meal simulation model includes glucose G and insulin I, with the glucose fluxes, i.e. rate of appearance (R_a), endogenous glucose production (EGP), glucose utilisation (U), renal extraction (E), and insulin fluxes, i.e. secretion (S) which is taken as zero for type-1 patient and degradation (D) [5]. The dynamic equations that represent the meal simulation model are given below.

8.1.1 Glucose intestinal absorption: Glucose intestinal absorption describes [5] the glucose transit through the stomach and intestine

$$\begin{aligned}
Q_{\text{sto}}(t) &= Q_{\text{sto1}}(t) + Q_{\text{sto2}}(t)\\
\dot{Q}_{\text{sto1}}(t) &= -k_{\text{gri}}Q_{\text{sto1}}(t) + d(t)\\
\dot{Q}_{\text{sto2}}(t) &= -k_{\text{gut}}(t, Q_{\text{sto}})Q_{\text{sto2}}(t) + k_{\text{gri}}Q_{\text{sto1}}(t)\\
\dot{Q}_{\text{gut}}(t) &= -k_{\text{abs}}Q_{\text{gut}}(t) + k_{\text{gut}}(t, Q_{\text{sto}})Q_{\text{sto2}}(t)\\
R_a(t) &= \frac{f k_{\text{abs}} Q_{\text{gut}}(t)}{\text{BW}}
\end{aligned}$$

where Q_{sto} (mg) is the amount of glucose in the stomach (solid phase, Q_{sto1} and liquid phase, Q_{sto2}), Q_{gut} (mg) is the glucose mass in the intestine, k_{gri} is the rate of grinding, k_{abs} is the rate constant of intestinal absorption, f is the fraction of intestinal absorption that actually appears in plasma, d (mg/min) is the rate of ingested glucose, BW (kg) is body weight, R_a (mg/kg/min) is the glucose rate of appearance in plasma, and k_{empt} is the rate constant of gastric emptying.

$$k_{\text{gut}}(t,\ Q_{\text{sto}}) = k_{\text{min}} + \frac{k_{\text{max}} - k_{\text{min}}}{2}\left\{\tan h\left[a\left(Q_{\text{sto}} - b\bar{D}(t)\right)\right] - \tan h\left[c\left(Q_{\text{sto}} - \text{d}\bar{D}(t)\right)\right] + 2\right\}$$

$$a = \frac{5}{2\bar{D}(t)(1-b)}, \quad c = \frac{5}{2\bar{D}(t)d}, \quad \bar{D}(t) = Q_{\text{sto}}(t) + \int_t^{t_f} \text{d}(\tau)\text{d}\tau$$

where t and t_f are the initial and final times of the last ingestion, respectively, while a, b, c, d, k_{max} and k_{min} are model parameters.

8.1.2 Glucose subsystem: Two compartment models are used to describe glucose kinetics [5]

$$\begin{aligned}
\dot{G}_P(t) &= \text{EGP}(t) + R_a(t) + K_2 G_t(t) - E(t) - U_{ii}(t) - K_1 G_P(t),\\
\dot{G}_t(t) &= K_1 G_P(t) - K_2 G_t(t) - U_{id}(t)
\end{aligned}$$

where G_p (mg/kg) and G_t (mg/kg) are the glucose masses in plasma and rapidly equilibrating tissues and in slowly equilibrating tissues, respectively, EGP is the endogenous glucose production (mg/kg/min), E (mg/kg/min) is the renal excretion, U_{ii} and U_{id} are the insulin-independent and -dependent glucose utilisations (GUs), respectively, (mg/kg/min), and k_1, k_2 are the rate parameters.

8.1.3 SC glucose kinetics: SC glucose concentration G_M (mg/dl) is obtained as

$$\dot{G}_M(t) = -k_{\text{sc}}G_M(t) + k_{\text{sc}}\frac{G_P(t)}{V_G}$$

where V_G (dl/kg) is the body weight-normalised glucose volume and k_{sc} is a rate constant.

8.1.4 Glucose renal excretion: Glucose excretion by the kidney occurs if plasma glucose exceeds a certain threshold and is modelled as

$$E(t) = \begin{cases} K_{e1}\left[G_p(t) - K_{e2}\right]; & \text{if } G_p(t) > K_{e2}\\ 0; & \text{if } G_p(t) \le K_{e2} \end{cases}$$

where K_{e1} (min^{-1}) is the glomerular filtration rate and K_{e2} is the renal threshold of glucose.

8.1.5 Endogenous glucose production: It comprises a direct glucose signal and a delayed insulin signal [5]

$$\begin{aligned}
\text{EGP}(t) &= k_{p1} - k_{p2}G_p(t) - k_{p3}I_d(t)\\
\text{EGP}(0) &= \text{EGP}_b
\end{aligned}$$

where delayed insulin signal I_d (pmol/l) is given by

$$\dot{I}_1(t) = -k_i\left[I_1(t) - I(t)\right],$$

$$\dot{I}_d(t) = -k_i\left[I_d(t) - I_1(t)\right],$$

$$I_1(0) = I_d(0) = I_b$$

where I (pmol/l) is the plasma insulin concentration, k_{p1} is the extrapolated EGP at zero glucose and insulin, k_{p2} is the liver glucose effectiveness, k_{p3} is a parameter governing the amplitude of insulin action on the liver, and k_i is the rate parameter accounting for the delay between insulin signal and insulin action.

8.1.6 Glucose utilisation: GU by body tissues during a meal consists of two components. One is insulin-independent GU $U_{ii}(t) = F_{cns}$. Another is insulin-dependent component $U_{id}(t)$ which depends non-linearly on glucose concentration in the tissues

$$U_{id}(t) = \frac{V_m(t)G_t(t)}{K_m + G_t(t)},$$
$$V_m(t) = V_{m0} + V_{mx}X(t),$$

$$\dot{X}(t) = -p_{2u}X(t) + p_{2u}[I(t) - I_b]$$

where K_m, V_{m0} and V_{mx} are model parameters; X (pmol/l) is the remote insulin signal; I_b is the basal insulin level; p_{2u} is the rate constant of the insulin action on peripheral glucose utilisation.

8.1.7 SC insulin kinetics: This work uses the variation of a model described in Nucci and Cobelli

$$\dot{I}_{\mathrm{sc1}}(t) = -(k_d + k_{a1})I_{\mathrm{sc1}}(t) + u(t),$$
$$\dot{I}_{\mathrm{sc2}}(t) = k_d I_{sc1}(t) + k_{a2}I_{\mathrm{sc2}}(t)$$

where I_{sc1} is the amount of non-monomeric insulin in the SC space, $I_{sc2}$is the amount of monomeric insulin in the SC space, $u(t)$ (pmol/kg/min) is the exogenous insulin infusion rate, k_d (min^{-1}) is the rate constant of insulin dissociation, and k_{a1} and k_{a2} are the rate constants of non-monomeric and monomeric insulin absorption, respectively.

8.1.8 Insulin subsystem: The two-compartment model is used to describe insulin kinetics and the model equations are

$$\dot{I}_l(t) = -(m_1 + m_3)I_l(t) + m_2 I_p(t),$$
$$\dot{I}_p(t) = -(m_2 + m_4)I_p(t) + k_{a1}I_{\mathrm{sc1}}(t) + k_{a2}I_{\mathrm{sc2}}(t),$$
$$I(t) = \frac{I_p(t)}{V_l}$$

where I_{sc1} is the amount of non-monomeric insulin in the SC space, I_{sc2} is the amount of monomeric insulin in the SC space, $u(t)$ (pmol/kg/min) is the exogenous insulin infusion rate, k_d (min^{-1}) is the rate constant of insulin dissociation, and k_{a1} and k_{a2} are the rate constants of non-monomeric and monomeric insulin absorption, respectively.